Optical study of a -plane InGaN/GaN multiple quantum wells with different well widths grown by metal-organic chemical vapor deposition

T. S. Ko, T. C. Lu, T. C. Wang, J. R. Chen, R. C. Gao, M. H. Lo, H. C. Kuo, S. C. Wang, and J. L. Shen

Citation: Journal of Applied Physics **104**, 093106 (2008); doi: 10.1063/1.3013435
View online: http://dx.doi.org/10.1063/1.3013435
View Table of Contents: http://scitation.aip.org/content/aip/journal/jap/104/9?ver=pdfcov
Published by the AIP Publishing

Optical study of *a*-plane InGaN/GaN multiple quantum wells with different well widths grown by metal-organic chemical vapor deposition

T. S. Ko,[1] T. C. Lu,[1,a)] T. C. Wang,[1] J. R. Chen,[1] R. C. Gao,[1] M. H. Lo,[1] H. C. Kuo,[1,a)] S. C. Wang,[1] and J. L. Shen[2]
[1]*Department of Photonics and Institute of Electro-Optical Engineering, National Chiao Tung University, 1001 Ta Hsueh Rd., Hsinchu 30050, Taiwan*
[2]*Physics Department, Chung Yuan Christian University, Chung-Li 32023, Taiwan*

(Received 1 February 2008; accepted 19 September 2008; published online 7 November 2008)

a-plane InGaN/GaN multiple quantum wells of different widths ranging from 3 to 12 nm grown on *r*-plane sapphire by metal-organic chemical vapor deposition were investigated. The peak emission intensity of the photoluminescence (PL) reveals a decreasing trend as the well width increases from 3 to 12 nm. Low temperature (9 K) time-resolved PL (TRPL) study shows that the sample with 3-nm-thick wells has the best optical property with a fastest exciton decay time of 0.57 ns. The results of cathodoluminescence and micro-PL scanning images for samples of different well widths further verify that the more uniform and stronger luminescence intensity distribution are observed for the samples of thinner quantum wells. In addition, more effective capturing of excitons due to larger localization energy E_{loc} and shorter radiative lifetime of localized excitons are observed in thinner well width samples in the temperature dependent TRPL. © *2008 American Institute of Physics*. [DOI: 10.1063/1.3013435]

I. INTRODUCTION

During the past few years, group III nitrides have attracted a great amount of attention because of their various applications in electronic and optoelectronic devices.[1–3] However, the wurtzite nitride materials have polarization electrostatic fields along the polar *c* direction that results in the spatial separation of electron and hole wave functions within quantum wells, inducing the quantum confined Stark effect.[4] Therefore, overcoming the built-in electric field is one of main challenges for improvement of light emission efficiency. Recently, growth along nonpolar orientations has been explored to eliminate such polarization effects including $[11\bar{2}0]$ *a*-plane GaN, both on $[10\bar{1}2]$ *r*-plane sapphire and *a*-plane SiC, as well as $[10\bar{1}0]$ *m*-plane GaN on [100] $LiAlO_2$ substrates.[5,6]

The optical characteristics of *c*-plane InGaN/GaN multiple quantum wells (MQWs) have been studied extensively.[7,8] Chakraborty *et al.*[9] investigated the effect of defect density on optical properties of *a*-plane InGaN/GaN grown on laterally epitaxially over grown *a*-plane GaN. However, the optical properties of *a*-plane InGaN/GaN MQWs are not fully understood, including the effects of the lack of the internal field and possible different growth parameters. In general, the defect amounts of *c*-plane GaN, threading dislocation density is about $10^7–10^8$ cm^{-2} which is less than that of both *a*- and *m*-plane GaN.[10] Typically, there is around the threading dislocation density of $10^9–10^{10}$ cm^{-2} for both *a*- and *m*-plane GaN structures.[11–13] Unlike most stacking faults are essentially generated and close to the nucleation layer for *c*-plane GaN,[14] on the contrary, the different types of the stacking faults which distributed the whole *a*-plane GaN structure. Therefore, since the interface roughness and treading dislocations in *a*-plane heterostructures are more complicated than those in *c*-plane heterostructures,[11] the luminescence mechanism requires further clarification of the dependence of the optical characteristics on the different InGaN/GaN quantum well widths. Though Craven *et al.*[15] investigated optical characteristics of *a*-plane GaN/AlGaN MQWs with different well widths, however, the issues related to well width dependence of *a*-plane InGaN/GaN MQWs including luminescence efficiency and time-resolved analysis of carriers have not yet been confirmed. In this paper, we report on optical characteristics of nonpolar *a*-plane InGaN/GaN MQWs with different well widths grown by metal-organic chemical vapor deposition (MOCVD) on *r*-plane sapphire substrates. The photoluminescence (PL) experiments showed different optical properties between samples of different widths. Our cathodoluminescence (CL) images and scanning microphotoluminescence (μ-PL) images show the surface emission map of the samples, revealing the relation between well width and surface emission of *a*-plane InGaN/GaN MQWs. Furthermore, the results of temperature dependent PL revealed the localization features clearly, and low temperature time-resolved PL (TRPL) measurements further identified the localization effects in these samples.

II. EXPERIMENTAL DETAILS

All epitaxial films were grown on *r*-plane sapphire by MOCVD. Trimethylgallium, trimethylindium, and ammonia were used as precursors for sources of Ga, In, and N in whole epitaxial process. A 30-nm-thick AlN nucleation layer and a 2-μm-thick bulk GaN layer were deposited. The detailed growth parameters were reported elsewhere.[16,17] Four samples with different well widths were grown for investi-

a)Authors to whom correspondence should be addressed. Electronic addresses: timtclu@mail.nctu.edu.tw and hckuo@mail.nctu.edu.tw.

gation. The MQW structure consisted of ten pairs of alternating GaN barriers and InGaN wells. $\omega/2\theta$ scans of x-ray diffraction at $[11\bar{2}0]$ were applied for each sample. The results were modeled by using software built into the XRD equipment, showing that the In composition of the quantum well was around 23%, that the GaN barrier was around 12 nm thick and that the approximate well width for each samples was 3, 6, 9, and 12 nm, respectively. After growing the MQWs, a 50 nm capping layer of GaN was deposited on each sample.

The spatially resolved CL imaging data were obtained by scanning emission microscopy using a fixed viewing scale. To obtain μ-PL mappings, we used scanning optical microscopy and pumped our samples by a 325 nm He–Cd laser operating at 25 mW in room temperature. μ-PL spatial and spectral resolutions were 1 μm and 1 nm, respectively. Room temperature PL measurements were also performed using the cw 325 nm He–Cd laser operating at an excitation level of 25 mW. Power-dependent PL measurements were carried out using power density ranging from $2-200$ mW/cm^2. After the above experiments, the samples were placed in a vacuum chamber of 1.3 Pa attached to a closed-cycle helium cryogenic chamber for further temperature dependent PL experiments between 20–300 K. In addition, TRPL measurements were performed between 9–300 K using time-correlated single-photon counting and a 396 nm pulsed GaN diode laser as the excitation source. According to the report by Jordan *et al.*,[18] the carrier density n_0 can be given by $n_0=0.68A(1\text{-}R)P/(\hbar\omega S\gamma)$, where $\hbar\omega$ is the photon energy, S is the excited area, and γ is the laser repetition rate. In our TRPL experiments, the average laser pumping power was 0.2 mW with a pulse width of 56 ps operated at 10 MHz. The spot diameter was around 200 μm. Taking into account the reflection coefficient $R=23\%$ and the absorption A on the order of 10^5 cm^{-1}, we can calculate the initial carrier density in our excitation condition to be around 1.3×10^{10} cm^{-2}. This pumped effective carrier density 1.3×10^{10} cm^{-2} was designed as the low excitation condition to prevent strong carrier-carrier scattering. The instrument response time of our time-correlated single-photon counting system is about 300 ps.

III. RESULTS AND DISCUSSION

A. PL characteristics and spatial emission distribution of *a*-plane InGaN/GaN MQWs

The cw PL spectra of these four samples measured at room temperature are shown in Fig. 1(a). The PL peak emission energy of the MQWs increased from 2.47 to 2.79 eV with the decreasing well width, which could be attributed to the quantum confinement effect.[19,20] The similarity of peak energies for the 9 and 12 nm samples was due to the weak quantum confinement effect for larger well widths. Figure 1(b) shows that the PL peak emission intensity decreased with the increase in InGaN well width. As the well width was increased beyond 6 nm, the PL intensity dropped more quickly.

We then analyzed different power dependences $I\sim P^{\alpha}$ for the samples of different well widths over a wide range of

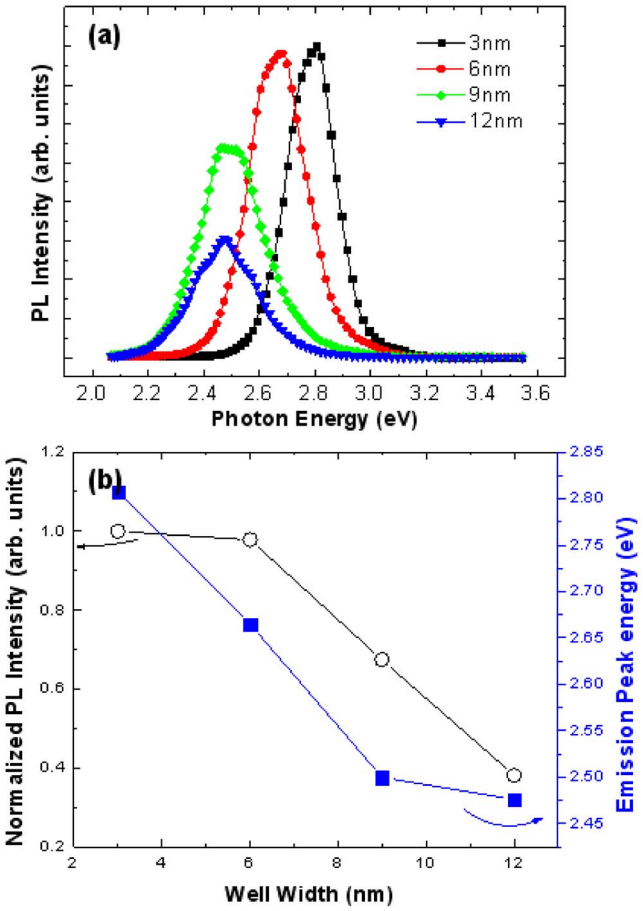

FIG. 1. (Color online) (a) Room temperature PL spectra of *a*-plane InGaN/GaN MQWs with well width ranging from 3–12 nm. (b) Normalized PL intensity and energy peak plotted as a function of quantum well width.

excitation power, where I is the PL intensity, P is the pumping power intensity, and α is the power index. In Fig. 2, the relationship between PL integrated intensity and excitation power density is observed. The respective inset figure reveals a full PL spectrum for all samples at room temperature. We have obtained unshifted PL peaks with increasing pumping power density, which is well known for *a*-plane hexagonal MQWs with the characteristic nonpolar flatband structure.[21] The power indices around 1 for our all samples both indicated that the radiative recombination dominated the optical transition[22] and gave additional evidence that no built-in electric field was present within any of our *a*-plane InGaN/GaN MQWs. However, such *a*-plane MQWs without the built-in electric field should not exhibit a large PL intensity dependence on the well width.[23] Other factors such as interface fluctuation, material quality, and carrier localization in the MQWs could play important roles in the PL emission intensity.

Figure 3 shows the CL and μ-PL emission images for the four samples using optical filters at the peak emission wavelength corresponding to each sample. The samples with thinner wells exhibited many, relatively large, and uniform luminescence patterns, indicating a higher crystal quality of their InGaN/GaN MQWs. In contrast, the sample with 12-nm-thick wells showed fewer and smaller luminescence patterns, demonstrating a high degree of inhomogeneity and re-

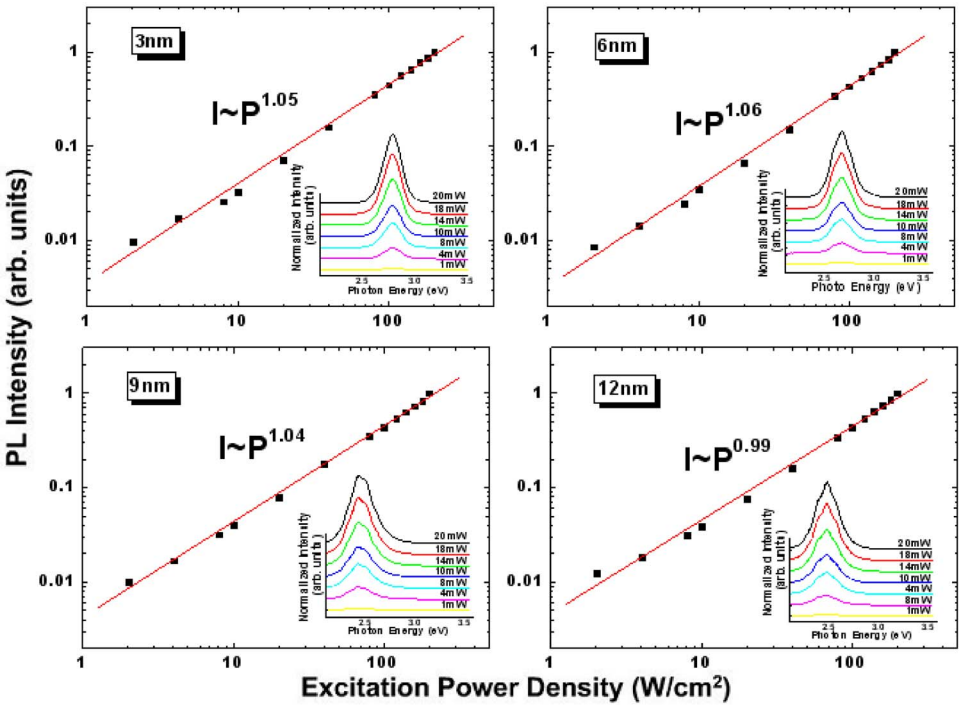

FIG. 2. (Color online) The relation between PL intensity and excitation power density for *a*-plane InGaN/GaN MQWs with different well widths. Inset images illustrate PL spectra as functions of the excitation power for the four *a*-plane InGaN/GaN MQWs with different well widths.

duced MQW crystal quality. These images revealed that the intensity of emission gradually decreases with increasing well width, which was consistent with the PL results. Such results were also similar to the results of μ-PL mapping shown in Fig. 3(b). In addition, atomic force microscopy (AFM) was applied for further identification of crystal quality. The results of plan-view AFM images indicated that the root mean square roughness gradually increased with increasing well width. The AFM result could give us additional proof that the crystal quality of MQWs improves when the well width was thinner. Accordingly, the CL images and μ-PL mapping would evidence that increasing well width increases more localized states and produces poor luminescence efficiency.

B. Localization features in *a*-plane InGaN/GaN MQWs

Figure 4 shows the evolution of the *a*-plane InGaN/GaN MQW PL spectra as a function of temperature from 20 to 300 K for each well width. The decrease in PL intensity with increasing temperature was observed. This thermal quenching PL intensity is a common phenomena in III-V semiconductor, which results from carriers' thermalization from either the radiative recombination centers or the localized states (or both) to the nonradiative recombination centers. In addition, three separated peaks appeared in the PL spectrum. The high-energy peak of 3.35 eV in all samples is attributed to the signal of bulk GaN. The middle energy peak of 2.8 eV was clearly present in the samples of 3 and 6 nm well widths, whereas this peak broadened and merged with the lowest-energy signal in the samples of 9 and 12 nm well widths. This energy peak could be attributed to the signal coming from shallow localized states. The lowest-energy signal came from the optical transition in deep localized states. Obviously, the PL emission from excitons in deep localized states dominates the luminescence from 20 K to room temperature, and the other two higher energy emissions suffer an apparent, rapid thermal quenching when the temperature increases. Since the exciton dynamics at shallow localized states is very sensitive to the lattice temperature, it is hard for excitons to remain stable in shallow localized states when the temperature increases.[24] Therefore, the excitons in the shallower localized states have higher probabilities of transferring to the nonradiative recombination centers or relaxing into the lower localized states, both of which would quench the emission from high-energy states.[25] Because the emission from shallow localized states decreased with increasing temperature, and then the efficient radiative recombination of excitons could occur mainly at deep localized states. For both samples with thinner well widths of 3 and 6 nm, the emission of excitons from one or several shallow localized states with one dominant energy level was apparent. In comparison, the emission from shallow localized states in the samples with well widths of 9 and 12 nm seemed to be broadened at all temperature regions, indicating that there could be many shallow localized states with different energy levels in the thicker QWs. The reasons for this phenomenon could be at-

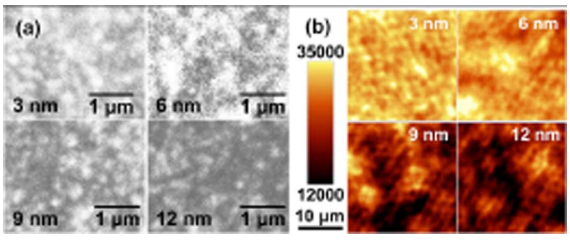

FIG. 3. (Color online) (a) Monochromatic top view CL images on samples of different well widths using optical filters at the corresponding peak emission wavelengths. (b) Top view μ-PL image of the same samples using optical filters at the corresponding peak emission wavelengths. The detected emission energies were 2.81, 2.67, 2.49, and 2.47 eV for the samples with 3, 6, 9, and 12 nm well widths, respectively.

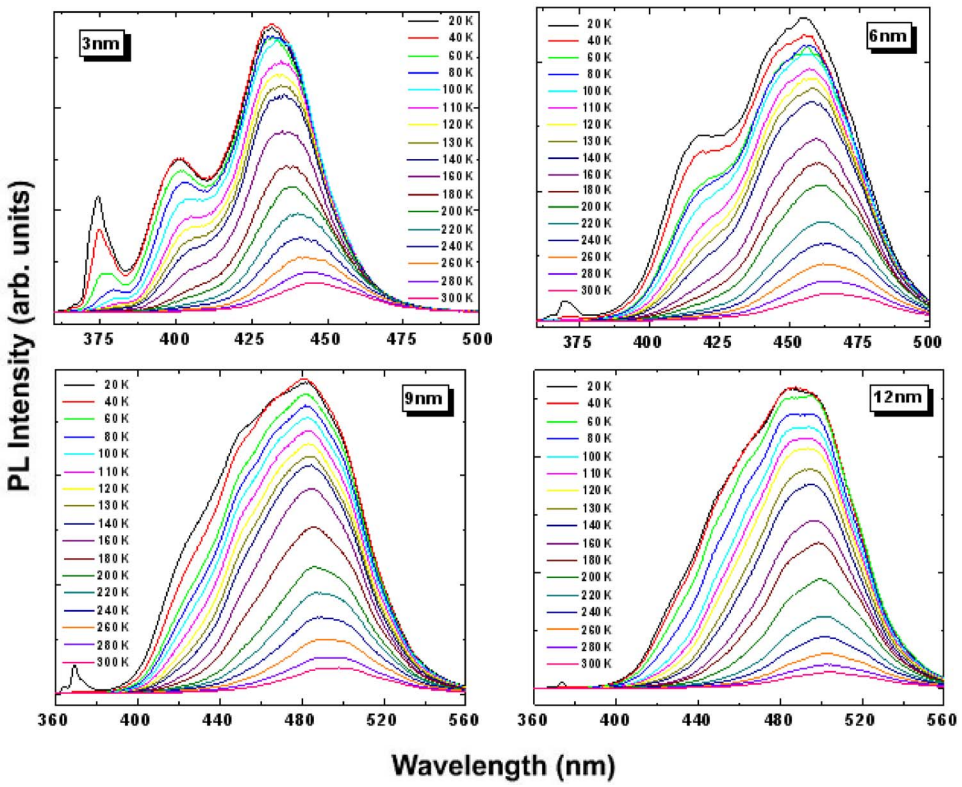

FIG. 4. (Color online) PL spectra as a function of temperature from 20 to 300 K for *a*-plane InGaN/GaN MQWs with different well widths.

tributed to two factors. One is that the In composition is not uniform especially in the thicker QWs, and thus more localization energy depths occur. The other factor is probably due to rough interfaces between well and barrier layers in MQW structure. The exciton energy can be defined as a function of x and L in the MQWs, which can be written as

$$E(x,L) = E_g(x) + E_c(L) + E_b, \tag{1}$$

where x is the In composition and L is the well thickness. The symbols, $E_g(x)$, $E_c(L)$, and E_b are the energy gap of InGaN well, confinement energy, and binding energy of the exciton in InGaN well, respectively. The well width L in Eq. (1) is a function of confinement energy of exciton. Different well widths L can influence the whole exciton energy $E(x,L)$. Therefore, the interface roughness in InGaN/GaN MQWs causes well width fluctuation, which leads to different confinement energies of exciton.[26] Note that the impact of interface roughness on $E_c(L)$ is more severe when the quantum well is thinner. Even 1 ML (monolayer) difference in the quantum well thickness will result in a large energy difference. On the other hand, when the quantum well thickness is thicker, the interface roughness will result in many small energy variations of $E_c(L)$, which could explain why broadened shallow localized states with different energy levels exist in the thicker QWs. Narukawa *et al.*[27] also pointed out the correlation between the interface roughness and alloy disorder in InGaN/GaN MQWs, attributing the broad PL spectra to not only In phase separation but also well width fluctuation.

In order to further check the degree of alloy and interface fluctuations in these four samples, we analyzed the peak shift of the InGaN MQW emission over the investigation temperature range as shown in Figs. 5(a)–5(d). For the samples with 3 and 6 nm well widths, the emission energy decreased monotonically with increasing temperature. However, for the samples with 9 and 12 nm well widths, the emission energy decreased at temperatures below 70 K, then increased with increasing temperature from 70 to around 140 K and finally decreased with further increase in temperature up to the room temperature. This redshift -blueshift -redshift of peak energy with increasing temperature is a famous characteristic of the exciton localization effect.[24,28] From 20 to 70 K, the observed dynamical redshift of the PL spectrum is considered to be caused by migration of excitons from higher states into lower localized states. At elevated temperature from 70 to 140 K, nonradiative recombination processes become more pronounced, and some carriers recombine before reaching deeper band-tail states, resulting in a blueshift in the PL peak position. At higher temperatures up to 300 K, another redshift occurs mainly due to the temperature dependent dilation of the lattice and electron-lattice interaction.[29,30] The total redshifts of the four samples over the temperature ranges used are 100, 75, 55, and 62 meV for 3, 6, 9, and 12 nm QW widths, respectively. The absence of S-curve characteristics for emission peak energies of 3 and 6 nm well widths could be due to a deeper localization depth for thinner wells, confining carriers tightly. Thus distinctively visible S-shaped temperature dependent behavior would not appear.[31] This is also consistent with our above inference that probably due to In phase separation and interface roughness.

C. Analysis of localization depth

Figure 6(a) shows the low temperature TRPL decay for samples with different well widths. Since the measurement was carried out at 9 K, the influence of the nonradiative

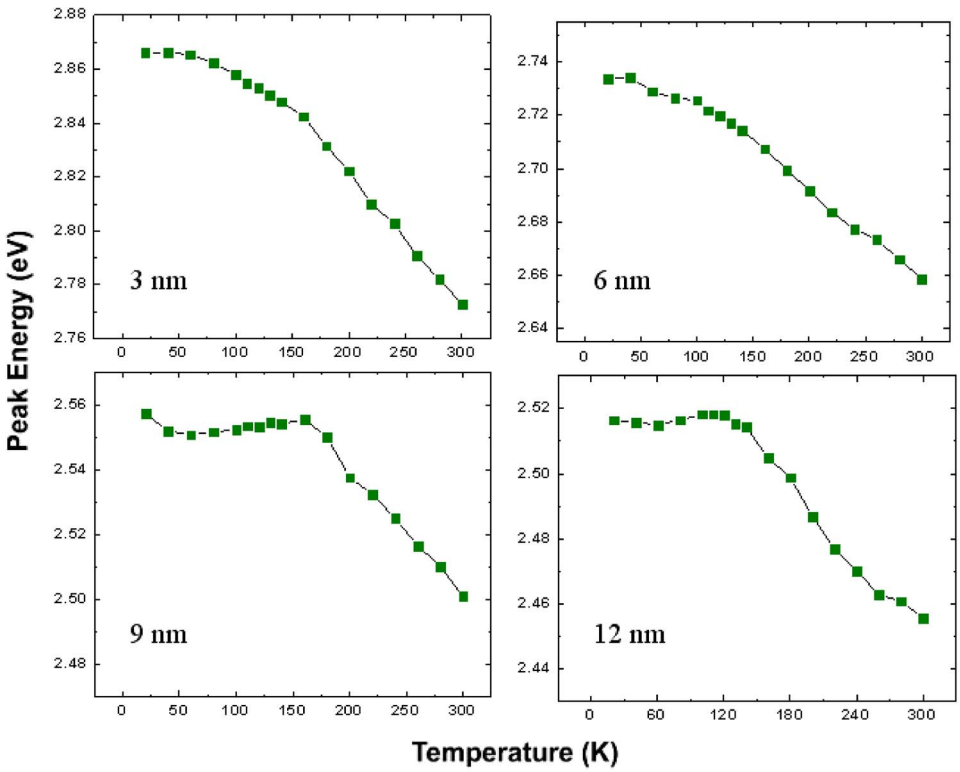

FIG. 5. (Color online) PL peak energy position as a function of temperature for *a*-plane InGaN/GaN MQWs with different well widths.

recombination process could be excluded.[32] All experiment data were fitted by a combined exponential and stretched exponential line shape $I(t)=I_1(0)\exp(-t/\tau_1)+I_2(0)\exp[-(t/\tau_2)^{\beta}]$, which has been used to analyze the emission characteristics of nonpolar InGaN/GaN MQWs.[32,33]

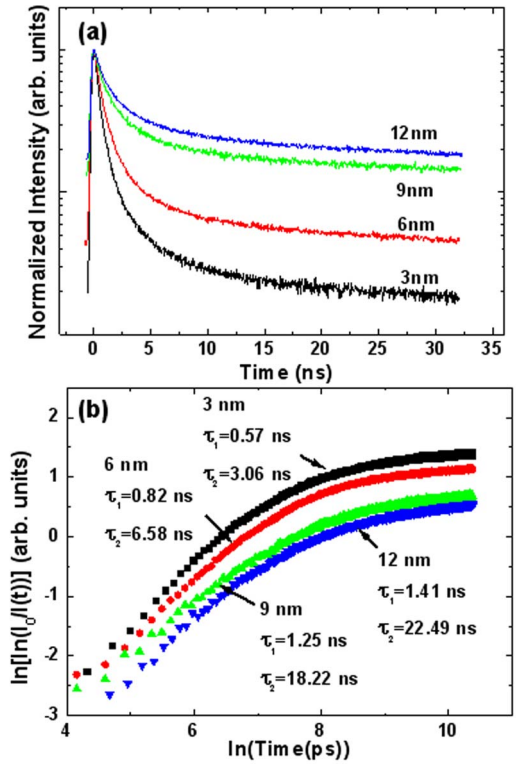

FIG. 6. (Color online) (a) TRPL signals of emission peaks in the *a*-plane InGaN/GaN MQWs with different well widths. (b) Relation between $\ln[\ln\{I(0)/I(t)\}]$ and $\ln(t)$ for the signal in (a).

The parameter $I(t)$ is the PL intensity at time t; β is the dimensionality of the localizing centers; τ_1 and τ_2 are the initial lifetimes of carriers. The fast decay time τ_1 ($\tau_1=0.57-1.41$ ns) represents the radiative recombination of free excitons in the extended states or localized states. The slow decay time τ_2 ($\tau_2=3.06-22.49$ ns) accounts for communication or relaxation of excitons between localized states. Figure 6(b) shows the relation between $\ln\{\ln[I(0)/I(t)]\}$ and $\ln(t)$ for the data in Fig. 6(a). We have obtained fast free exciton decay times τ_1 of 0.57 ns and the communication time τ_2 of 3.06 ns for the *a*-plane MQWs with 3 nm well width in comparison to the values of >6 ns reported for *c*-plane MQWs.[5] However, both of the PL decay times τ_1 and τ_2 detectably increased with the QW width as shown in Fig. 6. In general, growing a thick well using a long growth time could easily cause fluctuation of the In diffusion length and form worse interfaces between wells and barriers. Increasing the degree of In separation could result in more localized states in the MQWs. Therefore, more localized states in the thicker well could trap parts of carriers transitioning from higher levels to lower levels and further delay both lifetimes, τ_1 and τ_2. The longer exciton lifetime would decrease the PL emission intensity, which also explained the PL results of peak emission intensity as shown in Fig. 1(b).

We also analyze the decay time corresponding to different energies of the PL spectra at 9 K, which provides further evidence of the inhomogeneously broadened localization effect in these four samples. Figure 7 shows the PL decay time as a function of monitored photon energy at 9 K for the four samples. We attribute the circumstance to the existence of tail states.[34,35] The density of the tail states could be described as $\exp(-E/E_0)$, where E_0 represents the average of

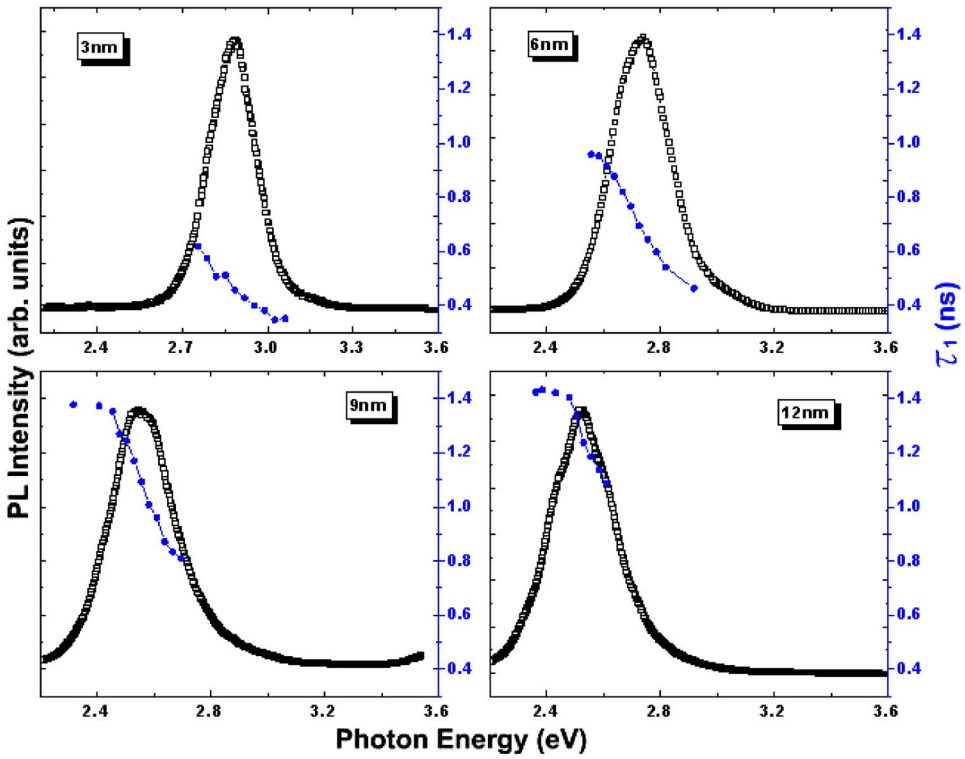

FIG. 7. (Color online) PL decay time as a function of monitored photon energy at 9 K (black) and the fitting data for the *a*-plane InGaN/GaN MQWs with different well widths (blue).

the depth difference between respective shallow localized centers and deep localized centers in the tail states. The PL decay time increases with decreasing monitored photon energy, which is characteristic of localized excitons in an exponential-tail density of states. The experimental results can be fitted[36]

$$\tau_{\mathrm{PL}}(E) = \tau_r/\{1 + \exp[(E - E_{\mathrm{me}})/E_0]\}, \tag{2}$$

where E_{me} is the energy of the absorption edge and τ_r is the effective lifetime. The resulting fitting parameters of the localization depth E_0 are 175, 71, 49, and 25 meV for 3, 6, 9, and 12 nm samples, respectively. The results show a deeper localization depth in thinner samples. Since the thermal energy is 26 meV at room temperature, excitons in the samples with thicker well widths could escape from an initial localized center with lower energy level to a higher one, creating a broader PL spectrum of such samples at room temperature. This result agrees well with the temperature dependent PL experiment.

D. Three-level localized exciton model

Chichibu *et al.* gave an explanation of the carrier transition mechanism for InGaN/GaN system as a simplified three-level schematic of a localized exciton system shown in Fig. 8.[37] In this model, excitons are transferred from the free/extended states to the localized states. The localization lifetime (τ_{loc}) is defined as the superposition of both the relaxation lifetimes of QW excitons transferring from free/extended states to localization centers and the radiative lifetime of localized excitons. τ_{loc} is a physical parameter which increases with temperature T and with the occupancy of the localization states, while it decreases with increasing in localization depth E_{loc}. We analyzed the radiative and nonradiative processes as a function of temperature for the four samples with different quantum well width. Values of the localization lifetime τ_{loc} and nonradiative lifetime in the free/extended states ($\tau_{\mathrm{nr,free}}$) are deduced from τ_{PL} and η_{int} (internal quantum efficiency) as a function of temperature using the relation

$$\eta_{\mathrm{int}} = 1/(1 + \tau_{\mathrm{loc}}/\tau_{\mathrm{nr,free}}),$$

$$1/\tau_{\mathrm{PL}} = 1/\tau_{\mathrm{loc}} + 1/\tau_{\mathrm{nr,free}}. \tag{3}$$

It is reasonable to assume that τ_{loc}, introduced in the three-level localized exciton model, combines with the superposition of τ_1 and τ_2 obtained in Fig. 5. Here we used the fast decay factor τ_1 to represent τ_{PL} because it dominated the PL intensity.[32] Internal quantum efficiency η_{int} can be estimated by using the ratio of temperature dependent integrated PL intensity between a given temperature T and the low temperature of 20 K.[38] The calculation results of $\tau_{\mathrm{nr,free}}$ and τ_{loc} are plotted in Fig. 9 by using Eq. (3). The τ_{loc} for all samples

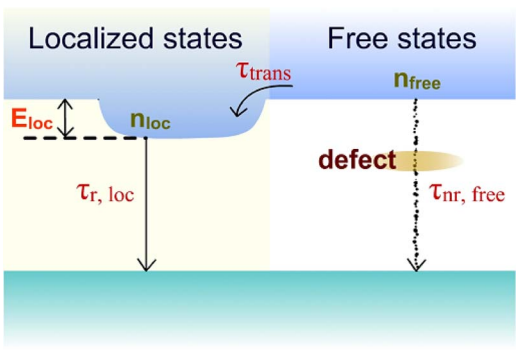

FIG. 8. (Color online) Schematic of the localized exciton system. Excitons are transferred from free/extended states to the localized states.

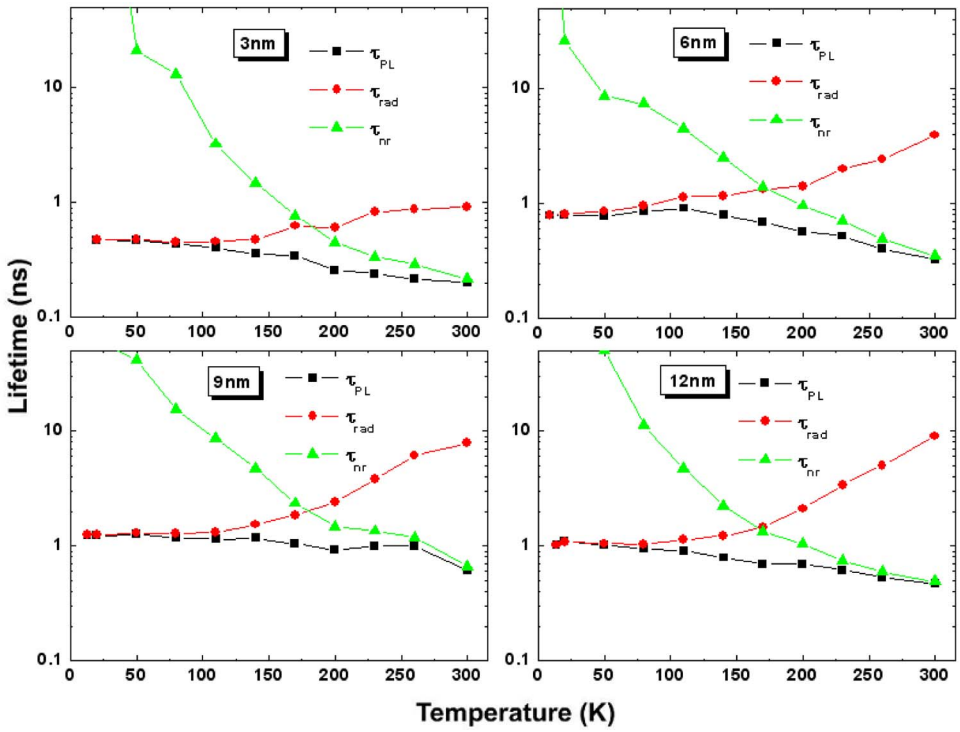

FIG. 9. (Color online) PL lifetime τ_{PL} of *a*-plane InGaN/GaN MQWs with different well widths as a function of temperature. The localization lifetime τ_{loc} and the nonradiative lifetime at the free/extended states $\tau_{nr,free}$, estimated from the temperature dependent TRPL signal and PL intensity are also plotted. The τ_{PL}, τ_{loc}, and $\tau_{nr,free}$ correspond to the definitions in the three-level localized exciton model shown in Fig. 8.

at low temperatures less than 100 K were around 1 ns, shorter than that of *c*-plane QWs, demonstrating the flatband feature of nonpolar QWs.[5] The τ_{loc} increased and the $\tau_{nr,free}$ decreased with increasing temperature, indicating that the efficiencies of the defect trapped excitons gradually strengthened as temperature rose. Therefore, once the temperature increased beyond 200 K, τ_{PL} was dominated by $\tau_{nr,free}$ in the four samples. On the other hand, τ_{loc} of the sample with the thinnest 3 nm well width at 300 K ($\sim$1 ns) was nine times shorter than that of the thickest 12 nm well width ($\sim$9 ns), which could be probably attributed to the difference in integrated intensity between the two samples. The $d\tau_{loc}/dT$ values indicate the abilities that localized centers trap and thermal activity for most excitons. At temperatures beyond 170 K, the $d\tau_{loc}/dT$ values were estimated as 3×10^{-3}, 2.5×10^{-2}, 5.6×10^{-2}, and 6.9×10^{-2} for the samples with well width of 3, 6, 9, and 12 nm, respectively. Samples with thinner well width had smaller $d\tau_{loc}/dT$ values, thus excitons were strongly localized and the thermal escape to two-dimensional spaces was suppressed.[31,32] As a result, shorter τ_{loc} and smaller $d\tau_{loc}/dT$ have indicated that effective capturing of excitons due to larger E_{loc} and/or shorter radiative lifetime of localized excitons was more prominent in thinner well width samples than thicker ones.[39]

IV. SUMMARY

In conclusion, ten pairs of *a*-plane InGaN/GaN MQWs of well width ranging from 3–12 nm grown by MOCVD on *r*-plane sapphire were investigated. The experimental results show both a stronger PL intensity and a wider emission CL and μ-PL area for samples with thinner well widths. The temperature dependent PL reveals that more uniform localization states, and all of the states have similar depth with similar depths for the samples with thinner well widths. In addition, more effective capturing of excitons due to larger localization energy E_{loc} and shorter radiative lifetime of localized excitons are observed in thinner well width samples by using temperature dependent TRPL. These phenomena are due to the better confinement of uniform and deep localized centers for excitons existing in the samples with thinner well widths, whereas more pronounced indium fluctuations or rougher interfaces in the MQWs exist in the samples with thicker well widths. These results should provide useful guidance for the fabrication of light emitting devices using *a*-plane InGaN/GaN MQW structures.

ACKNOWLEDGMENTS

We would like to thank Professor Y. F. Chen of National Taiwan University for CL support and C. D. Yerino of Yale University for proofreading this manuscript. This study was supported by the MOE ATU program and, in part, by the National Science Council of Taiwan, Republic of China under Contract Nos. NSC 96-2221-E009-092-MY3, NSC 96-2221-E009-093-MY3, and NSC 96-2221-E009-094-MY3.

[1] S. Nakamura and G. Fasol, *The Blue Laser Diode-GaN Based Light Emitters and Lasers* (Springer-Verlag, Berlin, 1997).
[2] S. Chichibu, T. Azuhata, T. Sota, and S. Nakamura, Appl. Phys. Lett. **69**, 4188 (1996).
[3] S. F. Chichibu, T. Sota, K. Wada, O. Brandt, K. H. Ploog, S. P. DenBaars, and S. Nakamura, Phys. Status Solidi A **183**, 91 (2001).
[4] F. Bernardini, V. Fiorentini, and D. Vanderbilt, Phys. Rev. B **56**, R10024 (1997).
[5] P. Waltereit, O. Brandt, A. Trampert, H. T. Grahn, J. Menniger, M. Ramsteiner, M. Reiche, and K. H. Ploog, Nature (London) **406**, 865 (2000).
[6] A. Chitnis, C. Chen, V. Adivarahan, M. Shatalov, E. Kuokstic, V. Mandavilli, J. Yang, and M. A. Khan, Appl. Phys. Lett. **84**, 3663 (2004).
[7] C. K. Sun, S. Keller, G. Gang, M. S. Minsky, J. E. Bowers, and S. P. DenBaars, Appl. Phys. Lett. **69**, 1936 (1996).
[8] C. K. Sun, S. Keller, T. L. Chiu, G. Wang, M. S. Minsky, J. E. Bowers, and S. P. DenBaars, IEEE J. Quantum Electron. **3**, 731 (1997).
[9] A. Chakraborty, S. Keller, C. Meier, B. A. Haskell, S. Keller, P. Waltereit,

S. P. DenBaars, S. Nakamura, J. S. Speck, and U. K. Mishra, Appl. Phys. Lett. **86**, 031901 (2005).
[10]S. C. Jain, M. Willander, J. Narayan, and R. Van Overstraeten, J. Appl. Phys. **87**, 965 (2000).
[11]M. D. Craven, S. H. Lim, F. Wu, J. S. Speck, and S. P. DenBaars, Appl. Phys. Lett. **81**, 469 (2002).
[12]D. N. Zakharov, L. W. Zuzanna, B. Wagner, Z. J. Reitmeier, E. A. Preble, and R. F. Davis, Phys. Rev. B **71**, 235334 (2005).
[13]T. Nagai, T. Kawashima, M. Imura, M. Iwaya, S. Kamiyama, H. Amano, and I. Akasaki, J. Cryst. Growth **298**, 288 (2007).
[14]X. H. Wu, L. M. Brown, D. Kapolnek, S. Keller, B. Keller, S. P. DenBaars, and J. S. Speck, J. Appl. Phys. **80**, 15 (1996).
[15]M. D. Craven, P. Waltereit, J. S. Speck, and S. P. DenBaars, Appl. Phys. Lett. **84**, 496 (2004).
[16]T. S. Ko, T. C. Wang, R. C. Gao, H. G. Chen, G. S. Huang, T. C. Lu, H. C. Kuo, and S. C. Wang, J. Cryst. Growth **300**, 308 (2007).
[17]T. S. Ko, T. C. Lu, T. C. Wang, M. H. Lo, J. R. Chen, R. C. Gao, H. C. Kuo, S. C. Wang, and J. L. Shen, Appl. Phys. Lett. **90**, 181122 (2007).
[18]C. Jordan, J. F. Donegan, J. Hegarty, B. J. Roycroft, S. Taniguchi, T. Hino, E. Kato, N. Noguchi, and A. Ishibashi, Appl. Phys. Lett. **74**, 3359 (1999).
[19]H. Teisseyre, C. Skierbiszewski, B. Łucznik, G. Kamler, A. Feduniewicz, M. Siekacz, T. Suski, P. Perlin, I. Grzegory, and S. Porowski, Appl. Phys. Lett. **86**, 162112 (2005).
[20]N. Akopian, G. Bahir, D. Gershoni, M. D. Craven, J. S. Speck, and S. P. DenBaars, Appl. Phys. Lett. **86**, 202104 (2005).
[21]P. Waltereit, O. Brandt, A. Trampert, H. T. Grahn, J. Mennlger, M. Ramsteler, M. Relche, and K. H. Ploog, Nature (London) **406**, 865 (2000).
[22]E. Kuokstis, C. Q. Chen, M. E. Gaevski, W. H. Sun, J. W. Yang, G. Simin, and M. A. Khan, Appl. Phys. Lett. **81**, 4130 (2002).
[23]C. Monier, A. Freundlich, and M. F. Vilela, J. Appl. Phys. **85**, 2713 (1999).
[24]Y. H. Cho, G. H. Gainer, A. J. Fischer, J. J. Song, S. Keller, U. K. Mishra, and S. P. DenBaars, Appl. Phys. Lett. **73**, 1370 (1998).
[25]Y. Kanemitsu, K. Tomita, D. Hirano, and H. Inouye, Appl. Phys. Lett. **88**, 121113 (2006).
[26]K. C. Zeng, M. Smith, J. Y. Lin, and H. X. Jiang, Appl. Phys. Lett. **73**, 1724 (1998).
[27]Y. Narukawa, Y. Kawakami, M. Funato, S. Fujita, and S. Nakamura, Appl. Phys. Lett. **70**, 981 (1997).
[28]A. Bell, S. Srinivasan, C. Plumlee, H. Omiya, F. A. Ponce, J. Christen, S. Tanaka, A. Fujioka, and Y. Nakagawa, J. Appl. Phys. **95**, 4670 (2004).
[29]R. Moglich and R. Rompe, Z. Phys. **119**, 492 (1942).
[30]J. Bardeen and W. Shockley, Phys. Rev. **80**, 72 (1950).
[31]Y. T. Moon, D. J. Kim, J. S. Park, J. T. Oh, J. M. Lee, Y. W. Ok, H. Kim, and S. J. Park, Appl. Phys. Lett. **79**, 599 (2001).
[32]T. Onuma, A. Chakraborty, B. A. Haskell, S. Keller, S. P. DenBaars, J. S. Speck, S. Nakamura, and U. K. Mishra, Appl. Phys. Lett. **86**, 151918 (2005).
[33]Y. J. Sun, O. Brandt, S. Cronenberg, S. Dhar, H. T. Grahn, K. H. Ploog, P. Waltereit, and J. S. Speck, Phys. Rev. B **67**, 041306 (2003).
[34]F. Yang, M. Wilkinson, E. Austin, and K. O'Donnell, Phys. Rev. Lett. **70**, 323 (1993).
[35]S. F. Chichibu, T. Azuhata, H. Okumura, A. Tackeuchi, T. Sota, T. Mukai, Appl. Surf. Sci. **190**, 330 (2002).
[36]Y. Narukawa, S. Saijou, Y. Kawakami, S. Fujita, T. Mukai, and S. Nakamura, Appl. Phys. Lett. **74**, 558 (1999).
[37]S. F. Chichibu, T. Onuma, T. Aoyama, K. Nakajima, P. Ahmet, T. Chikyow, T. Sota, S. P. DenBaars, S. Nakamura, T. Kitamura, Y. Ishida, and H. Okumura, J. Vac. Sci. Technol. B **21**, 1856 (2003).
[38]T. Koyama, T. Onuma, H. Masui, A. Chakraborty, B. A. Haskell, S. Keller, U. K. Mishra, J. S. Speck, S. Nakamura, and S. P. DenBaars, Appl. Phys. Lett. **89**, 091906 (2006).
[39]T. Onuma, Y. Uchinuma, E. K. Suh, H. J. Lee, T. Sota, and S. F. Chichibu, Jpn. J. Appl. Phys., Part 2 **42**, L1369 (2003).